

Pyrene-Based Y-shaped Solid-State Blue Emitters: Synthesis, Characterization, and Photoluminescence

Xing Feng,^[a] Jian-Yong Hu,^{*,[a, b]} Liu Yi,^[a] Nobuyuki Seto,^[a] Zhu Tao,^[c] Carl Redshaw,^[d, e] Mark R. J. Elsegood,^[f] and Takehiko Yamato^{*,[a]}

Abstract: A series of pyrene-based Y-shaped blue emitters, namely, 7-*tert*-butyl-1,3-diarylpyrenes **4** were synthesized by the Suzuki cross-coupling reaction of 7-*tert*-butyl-1,3-dibromopyrene with a variety of *p*-substituted phenylboronic acids in good to excellent yields. These compounds were fully characterized by X-ray crystallography, UV/Vis absorption and fluorescence spectroscopy, DFT calculations, thermogravimetric analysis, and differential scanning calorimetry. Single-crystal X-ray analysis revealed that the Y-shaped arylpyrenes exhibited a low degree of

π stacking owing to the steric effect of the bulky *tert*-butyl group in the pyrene ring at the 7-position, and thus, the intermolecular π - π interactions were effectively suppressed in the solid state. Despite the significantly twisted non-planar structures, these molecules still displayed efficient intramolecular charge-transfer emissions with clear

Keywords: luminescence • organic light-emitting devices • pyrenes • structure elucidation • structure–activity relationships

solvatochromic shifts on increasing solvent polarity. An intriguing fact is that all of these molecules show highly blue emissions with excellent quantum yields in the solid state. Additionally, the two compounds containing the strongest electron-accepting groups, CN (**4d**) and CHO (**4f**), possess high thermal stability, which, together with their excellent solid-state fluorescence efficiency, makes them promising potential blue emitters in organic light-emitting device applications.

Introduction

Since pioneering works on small-molecule organic light-emitting devices (OLEDs) were reported by Tang et al.,^[1] OLEDs have attracted increasing industrial and academic interest owing to their high technological potential for next-generation full-color flat panel displays and solid-state lighting.^[1–4] Despite investigations into various organic compounds (such as small molecules, conjugated polymers, and carbon nanotubes) for OLED applications, the design and synthesis of blue light-emitting compounds with satisfactory multifunctional properties for high-performance OLEDs remains a challenge. Moreover, understanding of the underlying structure–property relationships in such systems is a topic of ongoing interest.

Pyrene is one of the classical polycyclic aromatic hydrocarbons (PAHs), with a high fluorescence (FL) quantum yield in solution and efficient excimer emission.^[5–8] The tendency of pyrene and its derivatives to form excimers has been widely used in supramolecular design and for probing the structural properties of macromolecular systems. The excimer FL of pyrene and its derivatives has also been employed to detect guest molecules^[9] and sense environmental parameters.^[10] However, because the formation of π aggregates/excimers leads to an additional emission band at a longer wavelength and quenching of FL with low FL quantum yields at high concentration or in the solid state, the use of pyrene and its derivatives as red–green–blue

[a] X. Feng, Dr. J.-Y. Hu, L. Yi, N. Seto, Prof. T. Yamato
Department of Applied Chemistry
Faculty of Science and Engineering, Saga University
1 Honjo-machi, Saga 840-8502 (Japan)
Fax: (+81)952-28-8679
E-mail: yamatot@cc.saga-u.ac.jp

[b] Dr. J.-Y. Hu
Department of Organic Device Engineering
Yamagata University, Yonezawa
Yamagata 992-8510 (Japan)
E-mail: hujianyong@yz.yamagata-u.ac.jp

[c] Prof. Z. Tao
Department Key Laboratory of Macrocyclic
and Supramolecular Chemistry of Guizhou Province
Guizhou University, Guiyang
Guizhou, 550025 (P.R. China)

[d] Dr. C. Redshaw
School of Chemistry, University of East Anglia
Norwich, NR4 7JT (UK).

[e] Dr. C. Redshaw
Present address:
Department of Chemistry, University of Hull
Hull, HU6 7RX (UK)

[f] Dr. M. R. J. Elsegood
Chemistry Department, Loughborough University
Loughborough, LE11 3TU (UK)

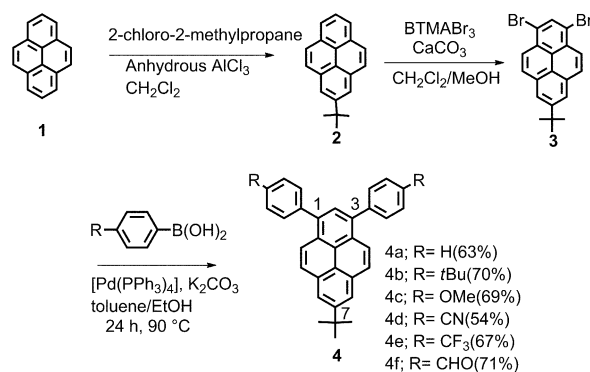
Supporting information for this article is available on the WWW under <http://dx.doi.org/10.1002/asia.201200530>. It contains additional characterization data (¹H and ¹³C NMR spectra of compounds **4** and **5**), crystal packing, and UV/Vis and fluorescence spectra of all compounds as well as quantum chemistry calculation results.

(RGB) emitters in OLED applications is still rather limited. To suppress the formation of pyrene dimers, many types of butterfly- and star-shaped molecules based on pyrene have been designed and synthesized for organic optoelectronic applications. Since the first example of a p-type organic field-effect transistor (OFET) based on butterfly-shaped pyrene-type molecules was reported by Zhu and co-workers,^[11] pyrene-based, star-shaped, organic semiconductors have been prepared for optoelectronic devices, such as OLED applications. For instance, Sonar and co-workers^[12] prepared 1,3,6,8-tetraaryl-functionalized pyrenes for applications in solution-processed organic electronic devices and the 1,3,6,8-tetrakis(4-butoxyphenyl)pyrene derivative as the active emitter showed high efficiencies with deep-blue emission, low turn-on voltages, and a maximum brightness. Thomas and co-workers developed new blue- to yellow-emitting materials by incorporating fluorene-based chromophores on the pyrene core with an acetylene linkage and using multifold palladium-catalyzed cross-coupling reactions.^[13] Both mono- and tetra-substituted alkynylpyrenes were tested as emitting dopants with the host material, 4,4-bis(9H-carbazol-9-yl)biphenyl (CBP), in multilayered OLEDs and exhibited bright blue or yellow electroluminescence. Chow and co-workers also developed a series of sterically inhibited, π -stacked 1,3,6,8-tetraarylpyrenes, which were explored as blue-emitting materials in OLEDs.^[14] Kim with co-workers investigated the two-photon absorption properties and charge-transfer (CT) dynamics of a series of covalently linked *N,N*-dimethylaniline (DMA) and pyrenyl derivatives.^[15,16] Kang and co-workers explored a series of deep-blue dopants through a Buchwald–Hartwig coupling reaction with *N*-phenyl-*p*-(*R*)-phenylamines and 1,6-dibromopyrene;^[17] here the emission colors can be controlled by introducing electron-donating or -withdrawing R groups. Sankararaman and Venkataramana reported a pyrene octaldehyde derivative that showed aggregation through strong $\pi\cdots\pi$ and C–H $\cdots\pi$ interactions in solution and in the solid state.^[18] Spectroscopic evidence suggested that the sum of the multiple $\pi\cdots\pi$ and C–H $\cdots\pi$ interactions could become significant and might have influenced the optical properties of materials. Gopidas and Suneesh examined the photoinduced electron-transfer processes in a 1,6-bis(phenylethynyl)pyrene–phenothiazine dyad (BPEP–PT) by using various techniques.^[19] In addition to these star-shaped 1,3,6,8-tetra-substituted pyrenes, Müllen’s group recently reported a remarkable poly-7-*tert*-butyl-1,3-pyrene^[20,21] as an effective blue emitter for OLEDs applications, in which the *t*Bu group played an important role for suppressing undesirable π -stacking interactions in the solid state. On the other hand, similar Y-shaped pyrene derivatives were synthesized for investigations into intramolecular excimer formation and delayed FL in triplet–triplet annihilation.^[22] Recently, to inhibit undesirable face-to-face π stacking in solution and in the solid state, our group reported two types of cruciform- and hand-shaped alkynyl-functionalized π -conjugated pyrenes.^[23,24] Single-crystal X-ray analysis indicated that the bulky *t*Bu group in the pyrene rings at the 2,7- or 7-positions

played a key role in inhibiting π -stacking interactions between neighboring pyrene units. Moreover, the multiple conjugation pathways could also be pivotal in creating interesting optoelectronic properties. Herein, we report the synthesis, characterization, and photophysical properties of a series of Y-shaped aryl-functionalized pyrenes. The aim of our study was two-fold as follows: 1) to investigate the relationship between molecular structure and photophysical properties; and 2) to explore how the substituted donating or accepting groups at the *para* position of the benzene ring opposite to the *t*Bu group affect both the crystal packing and the photophysical properties.

Results and Discussion

According to previous reports, 7-*tert*-butyl-1,3-dibromopyrene (**3**)^[20,21] can be synthesized from 2-*tert*-butylpyrene (**2**) with Br₂ at temperatures below –78 °C. However, the reaction conditions are hard to control and complex by-products are formed. Although the *t*Bu groups can be preferably used to obtain the 1,3-dibromopyrene selectively, electrophilic substitution of pyrene can occur at other positions, such as the 5- or 5,9-positions, by formylation and acetylation.^[25] Furthermore, the use of two *t*Bu groups (i.e., at the 2- and 7-positions) allows substitution at the 4-, 5-, 9-, and 10-positions of the pyrene molecule to occur.^[26,27] Herein, we report new, milder conditions for the bromination of **2** and the synthetic route is shown in Scheme 1. Pyrene was first



Scheme 1. Synthesis of pyrene derivatives **4a–4f**. BTMABr₃ = benzyltrimethylammonium tribromide.

mono-*tert*-butylated to afford the 2-*tert*-butylpyrene (**2**), which was then treated with BTMABr₃ (3.5 equiv) in dry CH₂Cl₂ at room temperature to give the desired 1,3-dibromopyrene **3** in good yield (76%). The 7-*tert*-butyl-1,3-bis(aryl)pyrenes **4** were synthesized from dibromide **3** with the corresponding arylboronic acid by the Suzuki cross-coupling reaction in good to excellent yields.

The chemical structures of the compounds **4** were confirmed by X-ray diffraction, ¹H/¹³C NMR spectroscopy, FTIR spectroscopy, MS, and elemental analysis (EA).

Table 1. Photophysical and electrochemical properties of Y-shaped molecules **4a–4f** and **5**.

Y-shaped molecule	λ_{\max} abs [nm]		λ_{\max} PL [nm] ^[c]		log ϵ [M ⁻¹ cm ⁻¹]	Stokes shift [nm]		$\Phi_{\text{soln}}^{\text{[d]}}$ Soln/thin film	$T_m^{\text{[e]}}$ [°C]	$T_d^{\text{[f]}}$ [°C]
	Soln ^[a]	Film ^[b]	Soln ^[a]	Film ^[b]		Soln ^[a]	Film ^[b]			
4a	360	368	396 (291)	452 (290)	4.54	36	84	0.38/0.42	186	322
4b	363	369	400 (292)	451 (290)	4.54	37	82	0.50/0.64	263	330
4c	362	372	402 (292)	450 (285)	4.51	40	78	0.56/0.58	167	173
4d	365	375	421 (291)	474 (288)	4.49	56	99	0.78/0.68	282	371
4e	360	370	403 (291)	456 (289)	4.52	43	86	0.67/0.69	215	287
4f	372	382	484 (291)	482 (293)	4.46	112	100	0.76/0.48	178	372
5	363	–	400 (292)	–	4.53	37	–	–	214	–

[a] Maximum absorption wavelength measured in dichloromethane at room temperature. [b] Measured in thin neat films. [c] The values in the parentheses are excitation wavelengths. PL = photoluminescence. [d] Measured in dichloromethane and neat thin films, respectively. [e] Melting temperature (T_m) obtained from DSC measurements. [f] Decomposition temperature (T_d) obtained from TGA.

Table 2. Summary of crystal data of Y-shaped molecules of **4a**, **4c**, **4d**, **4f**, and **5**.

Complex	4a	4c	4d	4f	5
formula	C ₃₂ H ₂₆	C ₃₄ H ₃₀ O ₂	C ₃₄ H ₂₄ N ₂	C ₃₄ H ₂₆ O ₂	C ₄₂ H ₃₈ O ₈
M_r	410.53	470.61	460.58	466.55	670.72
crystal system	triclinic	monoclinic	monoclinic	monoclinic	orthorhombic
space group	$P\bar{1}$	$P2_1/c$	$P2_1/c$	$P2_1/c$	$Pnma$
a [Å]	9.937(9)	18.815(14)	9.933(8)	16.8067(13)	13.298(5)
b [Å]	12.976(11)	15.629(11)	14.177(11)	15.1341(12)	31.064(12)
c [Å]	19.018(17)	8.851(6)	17.386(13)	9.7272(8)	8.702(3)
α [°]	100.097(10)	90.00	90.00	90.00	90.00
β [°]	93.575(10)	103.255(9)	100.539(12)	102.9103(13)	90.00
γ [°]	105.895(10)	90.00	90.00	90.00	90.00
V [Å ³]	2306(4)	2533(3)	2407(3)	2411.6(3)	3595(2)
Z	4	4	4	4	4
ρ_{calcd} [mgm ⁻³]	1.183	1.234	1.271	1.285	1.239
T [K]	293(2)	123	123	150(2)	100(2)
unique reflns	7951	5722	5427	6805	4204
obsd reflns	4110	4734	4856	5331	2585
parameters	578	330	328	328	252
$R(\text{int})$	0.0415	0.0640	0.0526	0.0287	0.0932
$R [I > 2\sigma(I)]^{\text{[a]}}$	0.0683	0.1034	0.0897	0.0453	0.0975
wR_2 (all data) ^[b]	0.2085	0.3036	0.2204	0.1325	0.3173
GOF on F^2	1.009	1.186	1.227	1.043	1.068

[a] Conventional R on F_{hkl} : $\sum ||F_o| - |F_c|| / \sum |F_o|$. [b] Weighted R on $|F_{hkl}|^2$: $\sum [w(F_o^2 - F_c^2)^2] / \sum [w(F_o^2)^2]^{1/2}$.

All results were consistent with the formation of the expected Y-shaped arylpyrenes **4**. All compounds are very soluble in common organic solvents, such as CH₂Cl₂, CHCl₃, tetrahydrofuran (THF), and toluene. The thermal properties of **4** were investigated by thermogravimetric analysis (TGA) and differential scanning calorimetry (DSC) measurements. The decomposition temperatures (T_d) of pyrenes **4a–f** were in the range of 173–372 °C, corresponding to a 5% weight loss. Key thermal data for these pyrene derivatives are summarized in Table 1.

X-ray Crystallography

Attempts to prepare crystals of **4b** and **4e** suitable for X-ray crystallography were unsuccessful; however, crystals of **4a**, **4c**, **4d**, and **4f** were obtained by slow evaporation of a mixture of dichloromethane/hexane at room temperature. Key crystallographic data are listed in Table 2; crystal structures of each molecule are shown in Figure 1.

The crystal structures of **4a**, **4c**, **4d**, and **4f** (Figure 1) are characterized by 2D layered structures involving C–H \cdots π bonds, π – π interactions, and hydrogen bonds. Although the terminal moieties are different, the architectures are almost identical to each other. However, some differences were found between **4f** and the others. Thus, we will describe the crystal structures in detail and attempt to interpret the effect of the molecular structure on the optical properties.

Compound **4a** crystallizes in the triclinic crystal system with space group $P\bar{1}$, whereas compounds **4c**, **4d**, and **4f** crystallize in the monoclinic crystal system (space group $P2_1/c$ for **4c**, **4d**, and **4f**). In the crystals,

the terminal moieties adopt a reasonably twisted conformation, with a dihedral angle (torsion angle) relative to the pyrene core falling in the range 44.2–79.0° for **4a**, 46.7–56.6° for **4c**, 52.9–54.7° for **4d**, and 38.8–43.6° for **4f**. The torsion angles between the central pyrene ring and the terminal aryl groups in the present structures are less than that in the crystal structure of 1,3,6,8-tetrakis(2,4,6-trimethylphenyl)pyrene (86.2–88.2°),^[10] which suggests that the terminal aryl groups do not contribute effectively toward suppressing intermolecular interactions in the solid state.

Our previous reports have shown that bulky *t*Bu groups substituted at the 2,7- or 7-positions of the pyrene ring can play a crucial role in pyrene systems.^[24,25] On one hand, the sterically bulky *t*Bu groups were used to suppress undesirable face-to-face π stacking in solution and in the solid state. On the other hand, the electron-donating *t*Bu group can also be beneficial for making the wavelength of absorption and FL emission less bathochromically shifted. Moreover, these twist angles with steric hindrance between the pyrene core and the terminal chromophore groups can effectively

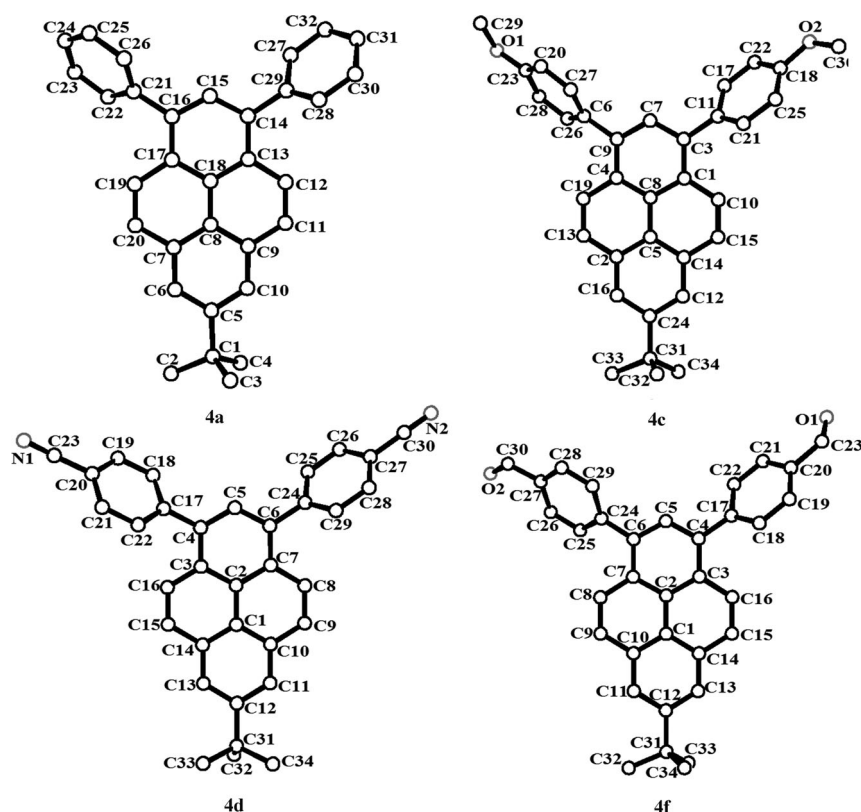


Figure 1. X-ray structures of compounds **4a**, **4c**, **4d**, and **4f**. Hydrogen atoms are omitted for clarity.

hinder tight intermolecular packing in the solid state. In compound **4a**, the molecules pack in a herringbone motif, as shown in Figure 2. Two neighboring pyrene moieties are present with displaced face-to-face patterns possessing a centroid to centroid distance of 5.52 Å and a slip angle of 28.1°, which is indicative of the existence of π - π interactions. Furthermore, there are three kinds of short C-H \cdots π (C61-H61 \cdots C18 = 2.96 Å, C55-H55 \cdots C21 = 3.34 Å, and C54-H54 \cdots C24 = 3.21 Å) noncovalent interactions present in the stacking structures. Arising from strong interactions of

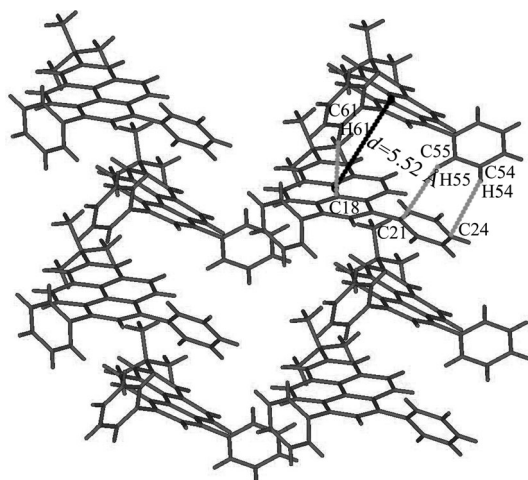


Figure 2. Crystal packing diagram of **4a** viewed down the *a* axis.

the phenyl ring with the adjacent pyrene core (C61-H61 \cdots C18 = 2.96 Å and \sphericalangle C61-H61-C18 = 157.2°), the terminal phenyl moieties are almost perpendicular to each other with an angle of 79.0° between the phenyl ring and the pyrene core.

Figure 3 shows the crystal packing for compound **4f**. Each molecule is arranged in a regular off-set geometry with C-H \cdots π (C25-H25 \cdots C1 = 2.88 Å, C34-H34 \cdots C9 = 2.85 Å and C21-H21 \cdots C28 = 2.68 Å) and hydrogen bond (C22-H22 \cdots O1 = 2.86 Å) noncovalent interactions along the *c* axis. The distance between pyrene centroids in neighboring molecules is 5.79 Å, which means that the stacking interactions between the pyrene moieties are rather weak. In comparison with **4a**, **4c**, and **4d**, possessing regular electron-withdrawing aldehyde

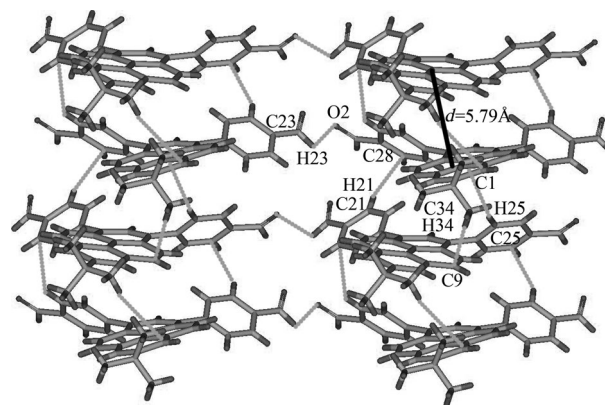


Figure 3. Crystal packing diagram of **4f** viewed parallel to the *c* axis.

groups, the molecular structure of compound **4f** is more planar with a smaller torsion angle between the phenyl group and the pyrene core; this increases π conjugation and delocalization of the electron density, which can be explained in terms of the noncovalent interaction between the pyrene rings that could lead to strong cooperative effects.^[28]

Photophysical Properties

The photophysical properties of the compounds **4** were examined both in dichloromethane and as films. All spectral data are summarized in Table 1. The UV/Vis absorption

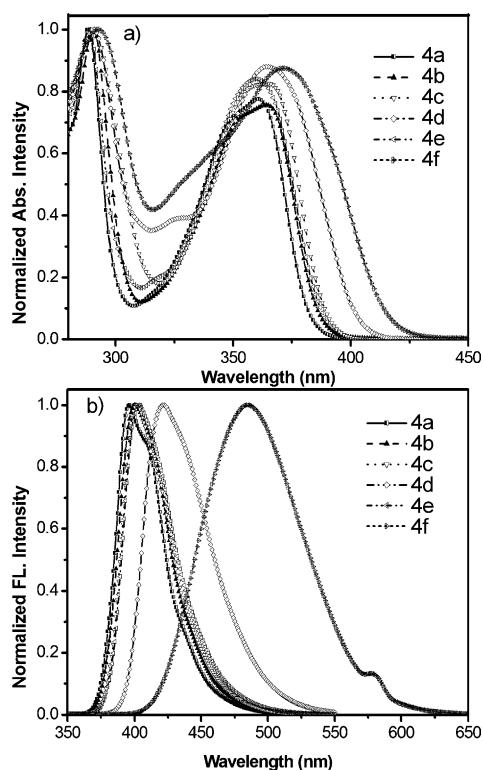


Figure 4. Normalized UV/Vis a) absorption and b) emission spectra of compounds **4a–f** recorded in dichloromethane at about 10^{-5} – 10^{-6} M at 25 °C.

spectra for **4**, recorded in dichloromethane, are shown in Figure 4a.

Compounds **4a–f** exhibit similar absorption behavior and two prominent absorption bands were observed in the regions $\lambda = 280$ – 295 and 360 – 375 nm. The short wavelength absorption located at $\lambda = 280$ – 295 nm revealed a vibronic feature for the unsubstituted parent pyrene and the higher energy absorption was associated with the intramolecular π – π^* transition. This absorption behavior is related to that observed for similar molecular structures with pyrene as the core. More interestingly, the absorption bands for compound **4f** were broader and larger red-shifts were observed at a λ_{max} of 293 and 372 nm. This was thought to be due to extended delocalization of the π electrons over a large area of the molecule, which was expected to broaden the absorption band and increase optical density.^[29] The intensities of the absorption bands exhibited the following order: CHO > CN > CF₃ > OMe > *t*Bu > H.

To further investigate the photophysical properties, the FL emission spectra for compounds **4** (Figure 4b) revealed that all pyrene derivatives emitted deep-blue emissions in the region of 370–450 nm, without observing any extra tailing absorption up to 550 nm; the exception was **4f**. All of the Y-shaped compounds exhibit bright-blue FL emissions, even at concentrations as low as 10^{-6} M. Compounds **4a**, **4b**, **4c**, **4d**, and **4e** exhibited a similar emission model, with band maxima located at 396, 400, 402, 421, and 403 nm in CH₂Cl₂, respectively. In the thin films, the emission absorp-

tion bands of **4** are significantly red-shifted by about 48–56 nm relative to those in solution (e.g., $\lambda_{\text{em}} = 452$ nm for **4a**, 451 nm for **4b**, 450 nm for **4c**, 474 nm for **4d**, and 456 nm for **4e**; Figure 5).

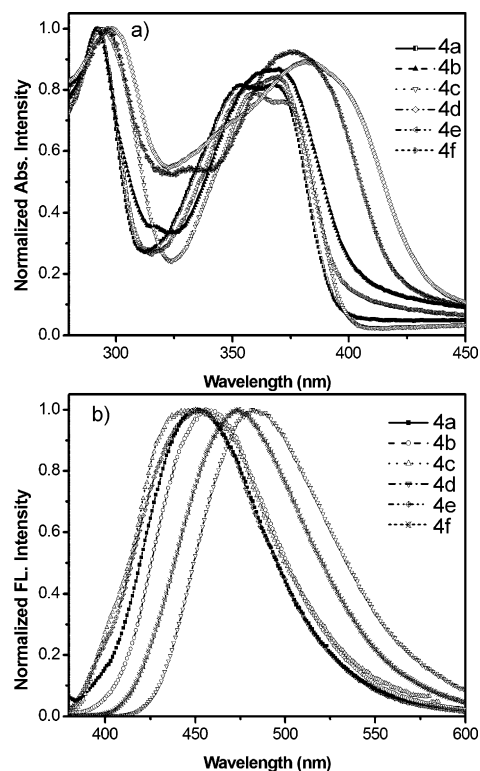


Figure 5. Normalized UV/Vis a) absorption and b) emission spectra of **4a–4f** in neat thin films.

This was consistent with the phenomena observed in the absorption spectra and ascribed to the effect of the substituents and intramolecular conformations of the similar Y-shaped pyrene derivatives. Additionally, the terminal arylphenyl substituents at the 6,8-position should barely hinder intermolecular interactions in the solid state owing to the small twist angle between the phenyl moieties and the pyrene core. However, the emission spectrum of **4f** exhibits a permanent broad absorption band with maximum emission peaks at 421 and 484 nm, which suggests that there are strong intermolecular interactions occurring in solution. Clearly, the bathochromic shift of the **4f** FL λ_{max} was larger than those for the compounds **4a**, **4b**, and **4c**. This can be ascribed to the terminal aldehyde groups, which can enlarge the π -conjugation length of the pyrene derivatives. Furthermore, the effects of concentration on the FL emissions of **4** were examined in CH₂Cl₂. Upon increasing the concentration from 3.0×10^{-8} to 5.0×10^{-4} M, the intensities of the emission band gradually increased and only the maximum absorption peak for the monomer were observed without extra excimer emissions (see Figure S6 in the Supporting Information). This evidence suggested that the attachment of the single bulky *tert*-butyl group at the 7-position could pre-

vent two Y-shaped molecules from getting close enough to result in excimer emission at high concentration and in the solid state. The quantum yield values, Φ_f , of **4** (Table 1) were recorded in solution (from 0.38 to 0.78) and in the thin film (from 0.42 to 0.69). In contrast, the PL spectrum of **4f** is about 2 nm blue-shifted in the solid state (≈ 482 nm) relative to that of the FL emission observed in solution (≈ 484 nm). The emission maxima of the films are located in similar regions to those observed in dichloromethane and tetrahydrofuran. This phenomenon suggests that the dielectric constant of compound **4f** in the solid film lies close to that in tetrahydrofuran and is less than that in dichloromethane.^[30,31]

The effects of solvent were investigated by using cyclohexane, THF, CH_2Cl_2 , CH_3CN , and *N,N*-dimethylformamide (DMF). The emission maxima of **4a–4c**, with electron-donating groups, were slightly shifted by up to 5 nm, depending on the solvent polarity. However, for compounds **4d–4f**, with electron-withdrawing groups, the solvent dependence in the emission spectra is remarkable, with large bathochromic shifts of 25 nm for **4d**, 10 nm for **4e**, and 75 nm for **4f**, (see Figure S7 in the Supporting Information). Figure 6 shows the normalized UV/Vis absorption and FL spectra for compound **4f** in various solvents. Because of the presence of CHO moieties, the absorption spectra of compound **4f** does not show any clear change, whereas the emission spectrum exhibits a more significant redshift in polar solvents than in nonpolar solvents from cyclohexane to DMF. This solvatochromism can be attributed to the decrease in energy

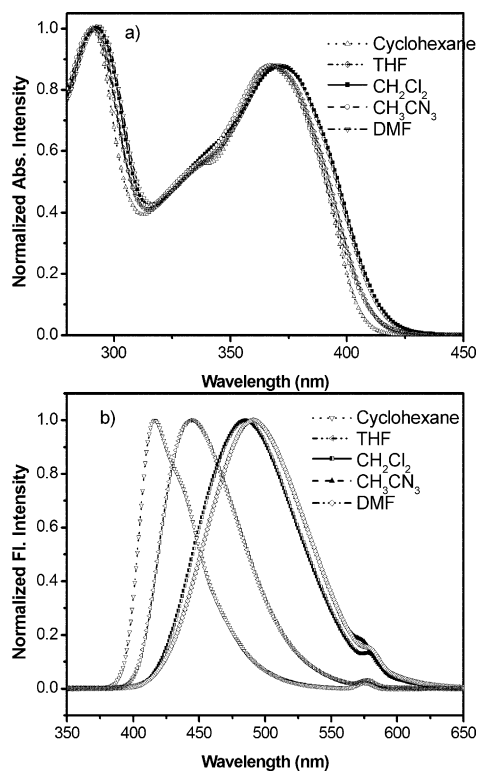
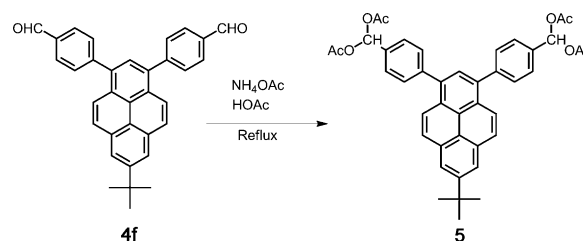


Figure 6. Normalized UV/Vis a) absorption and b) emission spectra of **4f** in cyclohexane, THF, CH_2Cl_2 , CH_3CN , and DMF at 25 °C.

of the singlet excited states as a function of increasing polarity of the solvents.^[32]

More importantly, the FL emission colors in solution strongly depended on the polarity of the solvents; for example, in cyclohexane, the FL of solution is deep blue, whereas in CH_2Cl_2 , DMF, or CH_3CN it is sky blue. We have also used a Lippert–Mataga plot to determine the line relationship of Stokes shift ($\Delta\nu_{st}$) against the solvent parameter $\Delta f(\epsilon, n)$ ^[33] (see Figure S8 in the Supporting Information).

To investigate the effects of the bulky block substitution groups in the pyrene ring on the geometric arrangements and the photophysical properties, we further prepared compound **5** from **4f**. This was achieved by an addition reaction with ammonium acetate (yield: 19%), in which two acetate groups were introduced at the *para* position of the benzene rings in the Y-shaped architecture to extend the terminal substitution group chains (Scheme 2).



Scheme 2. Synthetic route to compound **5**.

The chemical structure of **5** was initially determined on the basis of EA and spectral data. The ^1H NMR spectrum of **5** in CDCl_3 shows a singlet at $\delta = 2.20$ ppm for the methyl protons, a singlet at $\delta = 7.71$ ppm for the aromatic protons, and a singlet at $\delta = 7.82$ ppm for the methine protons. These data strongly support the proposed structure of **5**. A suitable crystal of **5** was obtained from a solution in a mixture of dichloromethane and acetone (1:1) by slow evaporation at room temperature. Low-temperature X-ray diffraction analysis revealed that compound **5** crystallized in the orthorhombic space group *Pnma* (Figure 7).

The asymmetric unit consists of half of the molecule, which lies on a mirror plane, with the terminal acetate units adopting a branched shape at the *para* position of each C_6H_4 aromatic ring. The torsion angle between the pyrene and C_6H_4 ring is 65.13° . The molecules of **5** adopt a 1D, slipped, face-to-face motif with off-set head-to-tail stacked columns, which contrasts with the herringbone structures observed for **4a**, **4c**, **4d**, and **4f**. The *t*Bu group is involved in a $\text{C} \cdots \text{H} \cdots \pi$ (C18–H18 \cdots C10) interaction with an intermolecular distance of 2.71 Å. There is some two-fold *t*Bu group disorder with an occupancy ratio 0.5:0.5 for C18, C19, and C20. However, there is no π stacking in this structure (see the Supporting Information) and this crystal structure demonstrates how the presence of the bulky *t*Bu group and an acetate group at the *para* position of the C_6H_4 rings can preclude the herringbone and stacking motifs found in most PAH structures.^[34]

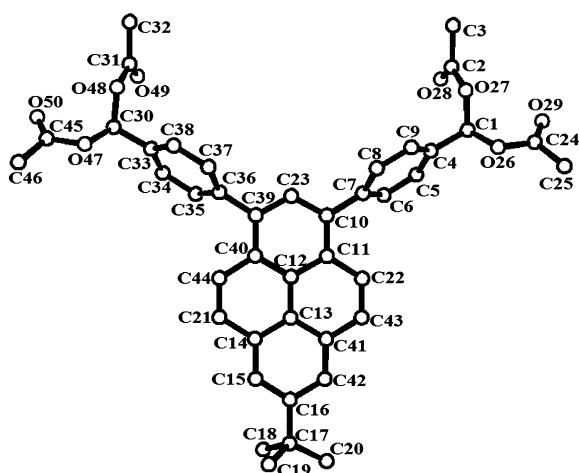


Figure 7. X-ray single-crystal structure of compound **5**. Hydrogen atoms are omitted for clarity.

The photophysical properties of compound **5** were investigated in dichloromethane. The UV/Vis absorption spectra of **5** have a sharp π - π^* transition centered at about 363 nm (Figure 8). The longest wavelength π - π^* band of **5** was hypsochromically shifted by about 9 nm in comparison to **4f**. This shift was due to the extended terminal acetate units replacing the carbaldehyde group of **4f**, thus saturating the sp^2

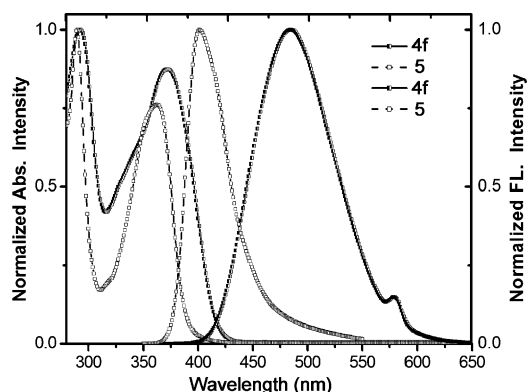


Figure 8. Normalized UV/Vis absorption (dashed lines) and emission (solid lines) spectra of **4f** and **5** in dichloromethane at about 10^{-5} – 10^{-6} M at 25 °C.

carbon to an sp^3 carbon center, which cut the LUMO-stabilizing donor–acceptor conjugation of **4f**. Similarly, the FL emission bands of **5** were also hypsochromically shifted by about 76 nm in comparison to that of **4f**. The results demonstrated that the presence of the *t*Bu group and extending the substituent chain efficiently suppressed π stacking in the structure and effectively influenced the photophysical properties.

Quantum Chemistry Computations

To obtain insight into the electronic structure of these aryl-functionalized pyrenes, DFT calculations (B3LYP/6-31G* basis set) were performed on **4a**–**4f** with the Gaussian 03W software package.^[35] The energies of the HOMO and LUMO levels for these compounds are collected in Table 3. The frontier orbital energies remain similar for all of the compounds; this indicates that the frontier orbitals are derived from the pyrene moieties in all compounds. The importance of the donor group on the pyrene ring is also attributed to the low-energy band, which allows a charge transfer (CT) transition between pyrene and phenyl segments. The HOMO–LUMO (H–L) energy gaps (ΔE) for all of the compounds were calculated to be in the range 3.32–3.54 eV (Figure 9), which was consistent with the first energy transition (350–375 nm).

Calculation of the theoretical maximum absorption values was consistent with the experimental values (360–372 nm). Similarly, the H–L energy gaps for these compounds suggests that the HOMO and LUMO are mainly comprised of the same pyrene core segment. The twist angle between the pyrene and phenyl group was also affected by the *para* substituents and followed the order CHO < CN < *t*Bu < OMe < CF₃ < H (based on optimized structural data, see the Supporting Information). The compounds are more planar with a smaller torsional angle, leading to extended delocalization of the π electrons over a large area of the molecule. The interplanar distance between the pyrene cores is longer, so that the π - π interactions are weakened by the substituents; thus broadening the absorption band and increasing the optical density, leading to stronger solid-state FL emission.

In addition, when investigating the effect of solvent polarity in cyclohexane, THF, CH₂Cl₂, CH₃CN, and DMF, only

Table 3. Computed frontier orbital energies for Y-shaped compounds **4a**–**4f**.

Compound	LUMO+1 [eV]	LUMO [eV]	HOMO [eV]	HOMO–1 [eV]	HOMO–LUMO ΔE [eV]	HOMO ^[a] [eV]	LUMO ^[b] [eV]	Energy gap ^[c] [eV]	Measured ^[d] λ_{\max} [nm]	Calcd λ_{\max} ^[e] [nm]
4a	–0.63	–1.55	–5.09	–5.99	3.54	–5.44	–2.20	3.24	360	350.8
4b	–0.57	–1.47	–5.01	–5.90	3.54	–5.48	–2.28	3.20	363	350.8
4c	–0.49	–1.41	–4.93	–5.71	3.32	–5.44	–2.27	3.17	362	374.1
4d	–1.63	–2.20	–5.61	–6.48	3.40	–5.69	–2.62	3.07	365	365.3
4e	–1.09	–1.90	–5.44	–6.31	3.51	–5.67	–2.51	3.16	360	353.8
4f	–1.85	–2.15	–5.47	–6.34	3.54	–5.67	–2.69	2.98	372	350.8
5	–0.82	–1.69	–5.22	–6.09	3.53				363	351.8

[a] Calculated from the empirical formula $HOMO = -(E_{ox} + 4.8)$. [b] $LUMO = HOMO + E_g$. [c] E_g estimated from UV/Vis absorption spectra. [d] Maximum absorption wavelength measured in dichloromethane at room temperature. [e] DFT (B3LYP/6-31G*) calculations were carried out with the use of structures optimized at the B3LYP/6-31G* level of theory.

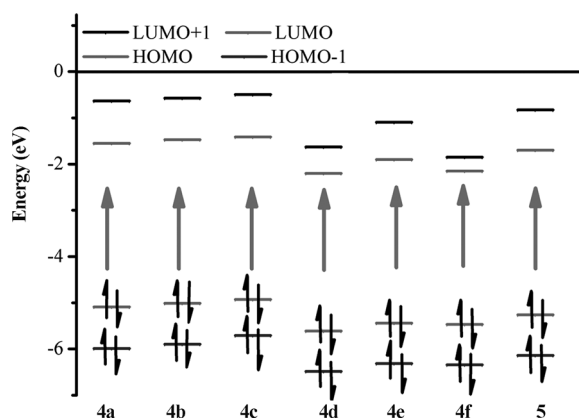


Figure 9. Schematic representations of HOMO–1, HOMO, LUMO, and LUMO+1 of **4** and **5**.

compounds **4d** and **4f** exhibit reasonable solvatochromism in the excited state. This suggests that peripheral electron-withdrawing groups, such as CHO (**4f**) and CN (**4d**), are necessary to impart CT character on the molecule. Their results are in good agreement with the DFT calculations. Furthermore, we also investigated the electrochemical characteristics of the pyrene derivatives **4** by cyclic voltammetry. The pyrenes were scanned positively and negatively, separately, in 0.10 M tetrabutylammonium perchlorate in anhydrous dichloromethane and THF with a scan rate of 100 mVs^{-1} at room temperature. All compounds **4** showed quasi-reversible or reversible processes (see the Supporting Information). In particular, compound **4c** in CH_2Cl_2 showed a quasi-reversible oxidation wave with half-wave potentials ($E_{\text{oxi}}^{1/2}$) at 1.43 V and an irreversible oxidation wave at a high oxidation potential 1.83 V (vs. the ferrocene couple Fc/Fc^+ ; see Table S3 in the Supporting Information). The HOMO and LUMO energy levels were evaluated by using the empirical formula $\text{HOMO} = -(E_{\text{ox}} + 4.8)$ from the on-set of the first oxidation. $\text{LUMO} = \text{HOMO} - E_g$, and the optical energy gap was derived from the lowest energy absorption onset in the absorption spectra. Values are listed in Table 3 and show that experimental data corresponds well with theoretical calculations.

Conclusion

We have synthesized a series of Y-shaped, pyrene-based, solid-state blue emitters by a Suzuki cross-coupling reaction using **3** in good to excellent yields. For the five crystal structures studied herein, the results revealed the effects of the substituent groups on the structures. Substitution at the *p*-positions of the benzene rings of the Y-shaped molecules can change the crystal structure and crystal-packing array. Depending on the electron-donating or -accepting groups and the length of the group, the Y-shaped arylpyrenes exhibit stable, soluble, and remarkable blue photophysical properties. Compounds **4a** and **4c**, with electron-donating groups, exhibited shifted face-to-face patterns with a slippage

angle. In compounds **4d** and **4f**, the electron-accepting groups, namely, cyano and aldehyde groups, enlarged the π -conjugation length and led to delocalization of electron density, and given that the phenyl moieties twisted with small angles, the trend was to form cofacial π - π stacking between adjacent pyrene cores. Compound **5**, with longer and flexible terminal moieties, effectively suppressed π - π stacking and led to an emission band in the deep-blue region. Compounds **4** and **5** have high blue FL emissions with high quantum efficiencies, good solubilities in common organic solvents, and high stabilities. Thus, on the basis of their excellent photophysical properties, these compounds are potentially useful as blue emitters for OLED applications.

Experimental Section

General

All melting points (Yanagimoto MP-S₁) are uncorrected. ^1H NMR spectra (300 MHz) were recorded on a Nippon Denshi JEOL FT-300 NMR spectrometer with SiMe_4 as an internal reference: *J* values are given in Hz. IR spectra were measured as KBr pellets in a Nippon Denshi JIR-AQ20M spectrophotometer. UV/Vis spectra were recorded on a Perkin-Elmer Lambda 19 UV/VIS/NIR spectrometer. Mass spectra were obtained on a Nippon Denshi JMS-01SA-2 spectrometer at 75 eV by using a direct-inlet system. EA was performed by using a Yanaco MT-5 instrument. Gas-liquid chromatography (GLC) analyses were performed by using a Shimadzu gas chromatograph, GC-14A; silicone OV-1, 2m; programmed temperature rise, $12^\circ\text{C min}^{-1}$; carrier gas nitrogen, 25 mL min^{-1} .

Materials

According to a reported method, compound **3**^[20] was synthesized from 2-*tert*-butylpyrene^[36] with Br_2 at a low temperature. The reaction conditions were hard to control to avoid the formation of complex by-products, so new milder conditions were explored and are shown in Scheme 1.

Synthesis of 2-*tert*-Butylpyrene (**2**)

A mixture of pyrene **1** (5 g, 24.2 mmol) and 2-chloro-2-methylpropane (2.62 g, 3.23 mL) was added to CH_2Cl_2 (40 mL) at 0°C and stirred for 15 min. Powdered anhydrous AlCl_3 (3.62 g, 27.2 mmol) was slowly added. The reaction mixture was continuously stirred for 3 h at room temperature and the reaction process was tracked by GC, then the solution was poured into a large excess of ice/water. The reaction mixture was extracted with dichloromethane ($2 \times 50 \text{ mL}$). The combined organic extracts were washed with water and brine, dried with anhydrous MgSO_4 , and the solvent was evaporated. The residue was recrystallized from hexane to afford pure 2-*tert*-butylpyrene (4.56 g, 71%) as a gray powder. Further recrystallization from hexane gave **2** as colorless prisms. M.p. 111.5 – 113.2°C (lit.^[36] M.p. 110 – 112°C). The ^1H NMR spectrum was in agreement with the reported values. ^1H NMR (300 MHz, CDCl_3): $\delta = 1.59$ (s, 9H; *t*Bu), 8.18 (d, $J = 9.2 \text{ Hz}$, 2H; pyrene-*H*), 8.30 (s, 2H; pyrene-*H*), 8.37 (d, $J = 9.2 \text{ Hz}$, 2H; pyrene-*H*), 8.47 ppm (s, 1H; pyrene-*H*).

Synthesis of 7-*tert*-Butyl-1,3-dibromopyrene (**3**)

A solution of BTMABr_3 (4.41 g, 3.5 mmol) in CH_2Cl_2 (20 mL) was added dropwise to a mixture of **2** (2.58 g, 1 mmol) and CaCO_3 (2 g, 20 mmol) in CH_2Cl_2 (30 mL) at 0°C for 1 h under argon atmosphere. The resulting mixture was allowed to slowly warm to room temperature and was stirred overnight. The reaction mixture was poured into ice water (60 mL) and neutralized with a 10% aqueous solution of $\text{Na}_2\text{S}_2\text{O}_3$. The mixture solution was extracted with dichloromethane ($2 \times 50 \text{ mL}$). The organic layer was washed with water ($2 \times 20 \text{ mL}$) and brine (20 mL), and then the solution was dried (MgSO_4) and condensed under reduced pressure. The crude compound was washed with hot hexane to afford **3**

(3.02 g, 76%) as a colorless solid. Recrystallization from hexane gave **3** as a gray solid. M.p. 199.5–201.2°C.

Synthesis of 1,3-Bisaryl-7-tert-butylpyrenes (**4**)

Compounds **4a–4f** were synthesized from **3** with the corresponding arylboronic acid by a Suzuki coupling reaction in high yield.

A mixture of **3** (200 mg, 0.5 mmol), 4-formylphenylboronic acid (300 mg, 2.0 mmol) in toluene (12 mL), and ethanol (4 mL) at room temperature was stirred under argon, and a 2 M aqueous solution of K_2CO_3 (20 mL) and $[Pd(PPh_3)_4]$ (70 mg, 0.06 mmol) were added. After the mixture was stirred for 30 min at room temperature under argon, the mixture was heated to 90°C for 24 h with stirring. After cooling to room temperature, the mixture was quenched with water, extracted with CH_2Cl_2 (3×100 mL), and washed with water and brine. The organic extracts were dried with $MgSO_4$ and the solvent was evaporated. The residue was purified by column chromatography eluting with (CH_2Cl_2/n -hexane, 1:1) to give **4f** as a white solid. Recrystallization from CH_2Cl_2/n -hexane (1:1) gave **4f** (166 mg, 71%) as a light-green powder. M.p. 178°C; 1H NMR (300 MHz, $CDCl_3$): δ = 1.60 (s, 9H; *t*Bu), 7.85 (d, J = 7.9 Hz, 4H; Ar-*H*), 7.92 (s, 1H; pyrene- H_2), 8.09 (d, J = 6.9 Hz; 4H; Ar-*H*), 8.11–8.14 (m, 4H; pyrene- $H_{4,5,9,10}$), 8.27 (s, 2H; pyrene- $H_{6,8}$), 10.16 ppm (s, 2H; CHO); ^{13}C NMR (75 MHz, $CDCl_3$): δ = 191.9, 149.8, 147.3, 135.6, 135.3, 131.3, 131.0, 129.8, 128.8, 128.2, 125.3, 124.3, 123.1, 123.0, 35.3, 31.9 ppm; IR (KBr): $\tilde{\nu}_{max}$ = 2960, 1699, 1602, 1564, 1462, 1388, 1360, 1306, 1207, 1167, 877, 843, 841, 822, 729, 602, 517 cm^{-1} ; MS: m/z : 466.2 [M] $^+$; elemental analysis calcd (%) for $C_{34}H_{26}O_2$ (466.0): C 87.52, H 5.62; found: C 87.21, H 5.56.

A similar procedure with phenyl boronic acid, 4-*tert*-butylphenylboronic acid, 4-methoxyphenylboronic acid, 4-cyanophenylboronic acid, and 4-trifluoromethylphenylboronic acid was followed for the synthesis of **4a–4e**.

7-*tert*-Butyl-1,3-diphenylpyrene (**4a**) was obtained as white prisms (recrystallized from CH_2Cl_2/n -hexane, 1:2; 124 mg, 63%). M.p. 186°C; 1H NMR (300 MHz, $CDCl_3$): δ = 1.59 (s, 9H; *t*Bu), 7.44–7.69 (m, 10H; Ar-*H*), 7.94 (s, 1H; pyrene- H_2), 8.01 (d, J = 9.2 Hz, 2H; pyrene- $H_{4,10}$), 8.18 (d, J = 9.2 Hz, 2H; pyrene- $H_{5,9}$), 8.20 ppm (s, 2H; pyrene- $H_{6,8}$); ^{13}C NMR (75 MHz, $CDCl_3$): δ = 149.2, 141.1, 137.1, 131.2, 130.6, 129.0, 128.3, 127.8, 127.6, 127.2, 125.3, 125.1, 123.4, 122.2, 35.2, 31.9 ppm; IR (KBr): $\tilde{\nu}_{max}$ = 2958, 2900, 2866, 1766, 1597, 1484, 1462, 1442, 1396, 1360, 1227, 1151, 875, 837, 810, 764, 702, 613, 503, 457 cm^{-1} ; MS: m/z : 410.2 [M] $^+$; elemental analysis calcd (%) for $C_{32}H_{26}$ (410.2): C 93.62, H 6.38; found: C 93.81, H 6.19.

7-*tert*-Butyl-1,3-bis(4-*tert*-butylphenyl)pyrene (**4b**) was obtained as a white powder (recrystallized from CH_2Cl_2/n -hexane, 1:3; 177 mg, 70%). M.p. 263°C; 1H NMR (300 MHz, $CDCl_3$): δ = 1.44 (s, 18H; Ar-*t*Bu), 1.59 (s, 9H; pyrene-*t*Bu), 7.56 (d, J = 8.6 Hz, 4H; Ar-*H*), 7.61 (d, J = 8.4 Hz, 4H; Ar-*H*), 7.97 (s, 1H; pyrene- H_2), 8.00 (d, J = 9.2 Hz, 2H; pyrene- $H_{4,10}$), 8.19 (s, 2H; pyrene- $H_{5,9}$), 8.23 ppm (d, J = 9.2 Hz, 2H; pyrene- $H_{6,8}$); ^{13}C NMR (75 MHz, $CDCl_3$): δ = 150.1, 149.1, 138.2, 137.1, 131.1, 130.3, 129.2, 127.6, 127.4, 125.4, 125.34, 123.5, 122.1, 35.2, 34.7, 31.9, 31.5 ppm; IR (KBr): $\tilde{\nu}_{max}$ = 2960, 1914, 1772, 1592, 1496, 1458, 1394, 1363, 1268, 1227, 1200, 1147, 1112, 1024, 877, 843, 810, 723, 665, 613, 567, 422 cm^{-1} ; MS: m/z : 522.3 [M] $^+$; elemental analysis calcd (%) for $C_{40}H_{42}$ (522.3): C 91.90, H 8.10; found: C 91.81, H 7.99.

7-*tert*-Butyl-1,3-bis(4-methoxyphenyl)pyrene (**4c**) was obtained as yellow prisms (recrystallized from CH_2Cl_2/n -hexane, 1:1; 113 mg, 69%). M.p. 167°C; 1H NMR (300 MHz, $CDCl_3$): δ = 1.58 (s, 9H; pyrene-*t*Bu), 7.10 (d, J = 8.8 Hz, 4H; Ar-*H*), 7.60 (d, J = 8.6 Hz, 4H; Ar-*H*), 7.91 (s, 1H; pyrene- H_2), 8.00 (d, J = 9.4 Hz, 2H; pyrene- $H_{4,10}$), 8.18 (d, J = 9.4 Hz, 2H; pyrene- $H_{5,9}$), 8.19 ppm (s, 2H; pyrene- $H_{6,8}$); ^{13}C NMR (75 MHz, $CDCl_3$): δ = 159.0, 149.1, 136.8, 133.5, 131.7, 131.2, 129.1, 127.6, 127.4, 125.4, 125.2, 123.5, 122.0, 113.8, 55.4, 35.2, 31.9 ppm; IR (KBr): $\tilde{\nu}_{max}$ = 2958, 1610, 1512, 1498, 1456, 1396, 1363, 1286, 1246, 1174, 1039, 877, 835, 727, 660, 607, 580, 553, 418 cm^{-1} ; MS: m/z : 470.2 [M] $^+$; elemental analysis calcd (%) for $C_{34}H_{30}O_2$ (470.2): C 86.77, H 6.43; found: C 86.53, H 6.41.

7-*tert*-Butyl-1,3-bis(4-cyanophenyl)pyrene (**4d**) was obtained as light-yellow prisms (recrystallized from CH_2Cl_2/n -hexane, 2:1; 120 mg, 54%). M.p. 282°C; 1H NMR (300 MHz, $CDCl_3$): δ = 1.60, (s, 9H; *t*Bu), 7.77 (d, J = 8.4 Hz, 4H; Ar-*H*), 7.83 (s, 1H; pyrene- H_2), 7.86 (d, J = 8.6 Hz, 4H;

Ar-*H*), 8.04 (d, J = 9.2 Hz, 2H; pyrene- $H_{4,10}$), 8.11 (d, J = 9.2 Hz, 2H; pyrene- $H_{5,9}$), 8.28 ppm (s, 2H; pyrene- $H_{6,8}$); ^{13}C NMR (75 MHz, $CDCl_3$): δ = 150.0, 145.6, 134.9, 132.3, 131.3, 131.0, 129.1, 128.2, 128.0, 125.3, 124.0, 123.3, 123.1, 118.8, 111.3, 35.3, 31.9 ppm; IR (KBr): $\tilde{\nu}_{max}$ = 2960, 2729, 1604, 1495, 1462, 1400, 1362, 1228, 1153, 877, 841, 816, 729, 661, 607, 559 cm^{-1} ; MS: m/z : 460.2 [M] $^+$; elemental analysis calcd (%) for $C_{34}H_{24}N_2$ (460.5): C 88.67, H 5.25, N 6.08; found: C 88.59, H 5.32, N 5.81.

7-*tert*-Butyl-1,3-bis(4-trifluoromethylphenyl)pyrene (**4e**) was obtained as colorless prisms (recrystallized from CH_2Cl_2/n -hexane, 1:1; 230 mg, 67%). M.p. 215°C; 1H NMR (300 MHz, $CDCl_3$): δ = 1.60 (s, 9H; *t*Bu), 7.78 (d, J = 8.4 Hz, 4H; Ar-*H*), 7.83 (d, J = 8.4 Hz, 4H; Ar-*H*), 7.88 (s, 1H; pyrene- H_2), 8.07 (d, J = 9.6 Hz, 2H; pyrene- $H_{4,10}$), 8.10 (d, J = 9.6 Hz, 2H; pyrene- $H_{5,9}$), 8.26 ppm (s, 2H; pyrene- $H_{6,8}$); ^{13}C NMR (75 MHz, $CDCl_3$): δ = 149.8, 144.6, 135.5, 131.0, 130.9, 129.8, 129.4, 128.6, 128.4, 128.2, 126.1, 125.5, 125.4, 125.3, 124.4, 123.2, 122.9, 122.5, 35.3, 31.9 ppm; IR (KBr): $\tilde{\nu}_{max}$ = 2958, 1616, 1326, 1167, 1122, 1062, 1015, 845, 724, 614, 508, 472 cm^{-1} ; MS: m/z : 546.2 [M] $^+$; elemental analysis calcd (%) for $C_{34}H_{24}F_6$ (546.2): C 74.72, H 4.43; found: C 74.61, H 4.05.

Synthesis of 7-*tert*-Butylpyrene-1,3-bis(4-carbaldehyde tetraacetate) (**5**)

A mixture of **4f** (46.7 mg, 0.1 mmol), ammonium acetate (308.4 mg, 4 mmol), and glacial acetic acid (10 mL) was heated at reflux for 5 h and then cooled to room temperature. The mixture was quenched with a 10% aqueous solution of $NaHCO_3$, which was then extracted with dichloromethane (2×50 mL). The organic layer was washed with water (2×20 mL) and brine (20 mL), the solution was dried ($MgSO_4$), and condensed under reduced pressure. The crude compound was purified by column chromatography eluting with (CH_2Cl_2 /acetone, 3:1) to give **5** as a yellow solid (13 mg, 19%). M.p. 214°C; 1H NMR (300 MHz, $CDCl_3$): δ = 1.59 (s, 9H; *t*Bu), 2.20 (s, 12H; Me), 7.71 (s, 8H; Ar-*H*), 7.82 (s, 2H; CH), 7.89 (s, 1H; pyrene- H_2), 8.03 (d, J = 9.2 Hz, 2H; pyrene- $H_{4,10}$), 8.14 (d, J = 9.2 Hz, 2H; pyrene- $H_{5,9}$), 8.22 ppm (s, 2H; pyrene- $H_{6,8}$); ^{13}C NMR (75 MHz, $CDCl_3$): δ = 168.9, 142.6, 136.2, 134.5, 131.1, 130.9, 127.9, 126.8, 125.3, 122.6, 122.5, 89.8, 89.7, 35.2, 31.9, 31.8, 21.0, 20.9 ppm; IR (KBr): $\tilde{\nu}_{max}$ = 3465, 2974, 1756, 1630, 1371, 1249, 1218, 1072, 1009, 974, 943, 836, 730, 607, 568, 524, 466 cm^{-1} ; MS: m/z : 670.11 [M] $^+$; elemental analysis calcd (%) for $C_{34}H_{24}F_6$ (670.75): C 75.21, H 5.71; found: C 75.02, H 5.83.

Crystal Data and Refinement Details for **4a**, **4c**, **4d**, **4f**, and **5**

Crystallographic data for compounds **4a**, **4c**, **4d**, **4f**, and **5** (see Table 2) were collected on SMART ApexII CCD^[37,38] or Rigaku Saturn 724 diffractometers with $Mo_{K\alpha}$ radiation (λ = 0.71073 Å). Structure solution and refinement were routine, except for **5**, in which the *t*Bu group was modeled with 50/50 disorder of the three methyl groups. Data (excluding structure factors) on the structures reported here have been deposited with the Cambridge Crystallographic Data Centre with deposition numbers CCDC 879770 (**4a**), 879771 (**4c**), 879772 (**4d**), 884805 (**4f**), and 879773 (**5**). These data can be obtained free of charge from the Cambridge Crystallographic Data Centre via www.ccdc.cam.ac.uk/data_request/cif.

Acknowledgements

This work was performed under the Cooperative Research Program of “Network Joint Research Center for Materials and Devices (Institute for Materials Chemistry and Engineering, Kyushu University)”. We would like to thank the OTEC at Saga University and the International Collaborative Project Fund of Guizhou province at Guizhou University for financial support. We also would like to thank the EPSRC (overseas travel grant to C.R.) and The Royal Society for financial support.

[1] C. W. Tang, S. A. VanSlyke, *Appl. Phys. Lett.* **1987**, *51*, 913–915.

- [2] Y. R. Sun, N. C. Giebink, H. Kanno, B. W. Ma, M. E. Thompson, S. R. Forrest, *Nature* **2006**, *440*, 908–912.
- [3] F. So, J. Kido, P. Burrows, *MRS Bull.* **2008**, *33*, 663–669.
- [4] S. Reineke, F. Linder, G. Schwartz, N. Seidler, K. Walzer, B. Lussem, K. Leo, *Nature* **2009**, *459*, 234–238.
- [5] T. M. Figueira-Duarte, K. Müllen, *Chem. Rev.* **2011**, *111*, 7260–7314.
- [6] J.-Y. Hu, T. Yamato, *Organic Light Emitting Diode – Material, Process and Devices, InTech*, Ed. S.-H. Ko, Croatia, **2011**, pp. 21–60.
- [7] J.-Y. Hu, Y.-J. Pu, G. Nakata, S. Kawata, H. Sasabe, J. Kido, *Chem. Commun.* **2012**, *48*, 8434–8436.
- [8] T. Förster, K. Z. Kasper, *Electrochem.* **1955**, *59*, 976–982.
- [9] D. Li, J. Song, P.-C. Yin, S. Simotwo, A. J. Bassler, Y.-Y. Aung, J. E. Roberts, K. I. Hardcastle, C. L. Hill, T. Liu, *J. Am. Chem. Soc.* **2011**, *133*, 14010–14016.
- [10] X.-L. Ni, S. Wang, X. Zeng, Z. Tao, T. Yamato, *Org. Lett.* **2011**, *13*, 552–555.
- [11] H.-J. Zhang, Y. Wang, K. Z. Shao, Y. Q. Liu, S. Y. Chen, W. F. Qiu, X. B. Sun, T. Qi, Y. Q. Ma, G. Yu, Z. M. Su, D. B. Zhu, *Chem. Commun.* **2006**, 755–757.
- [12] P. Sonar, M. S. Soh, Y. H. Cheng, J. T. Henssler, A. Sellinger, *Org. Lett.* **2010**, *12*, 3292–3295.
- [13] K. R. J. Thomas, N. Kapoor, M. N. K. P. Bolisetty, J.-H. Jou, Y.-L. Chen, Y.-C. Jou, *J. Org. Chem.* **2012**, *77*, 3921–3932.
- [14] J. N. Moorthy, P. Natarajan, P. Venkatakrishnan, D.-F. Huang, T. J. Chow, *Org. Lett.* **2007**, *9*, 5215–5218.
- [15] J. Sung, P. Kim, Y. O. Lee, J. S. Kim, D. Kim, *J. Phys. Chem. Lett.* **2011**, *2*, 818–823.
- [16] H. M. Kim, Y. O. Lee, C. S. Lim, J. S. Kim, B. R. Cho, *J. Org. Chem.* **2008**, *73*, 5127–5130.
- [17] K.-R. Wee, H.-C. Ahn, H.-J. Son, W.-S. Han, J.-E. Kim, D. W. Cho, S. O. Kang, *J. Org. Chem.* **2009**, *74*, 8472–8475.
- [18] G. Venkataramana, S. Sankararaman, *Org. Lett.* **2006**, *8*, 2739–2742.
- [19] C. V. Suneesh, K. R. Gopidas, *J. Phys. Chem. C* **2010**, *114*, 18725–18734.
- [20] T. M. Figueira-Duarte, P. G. Del Rosso, R. Trattnig, S. Sax, E. J. W. List, K. Müllen, *Adv. Mater.* **2010**, *22*, 990–993.
- [21] T. M. Figueira-Duarte, S. C. Simon, M. Wagner, S. I. Druzhinin, K. A. Zachariasse, K. Müllen, *Angew. Chem.* **2008**, *120*, 10329–10332; *Angew. Chem. Int. Ed.* **2008**, *47*, 10175–10178.
- [22] A. C. Benniston, A. Harriman, S. L. Howell, C. A. Sams, Y.-G. Zhi, *Chem. Eur. J.* **2007**, *13*, 4665–4674.
- [23] J.-Y. Hu, M. Era, M. R. J. Elsegood, T. Yamato, *Eur. J. Org. Chem.* **2010**, 72–79.
- [24] J.-Y. Hu, X.-L. Ni, X. Feng, M. Era, M. R. J. Elsegood, S. J. Teat, T. Yamato, *Org. Biomol. Chem.* **2012**, *10*, 2255–2262.
- [25] J.-Y. Hu, A. Paudel, T. Yamato, *J. Chem. Res.* **2008**, 308–311.
- [26] T. Yamato, A. Miyazawa, M. Tashiro, *J. Chem. Soc. Perkin Trans. 1* **1993**, 3127–3137.
- [27] T. Yamato, M. Fujimoto, A. Miyazawa, K. Matsuo, *J. Chem. Soc. Perkin Trans. 1* **1997**, 1201–1207.
- [28] A. Frontera, D. Quiñero, A. Costa, P. Ballester, P. M. Deyà, *New J. Chem.* **2007**, *31*, 556–560.
- [29] K. R. J. Thomas, J. T. Lin, Y.-T. Tao, C.-H. Chuen, *Chem. Mater.* **2002**, *14*, 3852–3859.
- [30] K. R. J. Thomas, J. T. Lin, Y.-T. Tao, C.-H. Chuen, *Chem. Mater.* **2002**, *14*, 2796–2802.
- [31] P. Tyagi, A. Venkateswararao, K. R. J. Thomas, *J. Org. Chem.* **2011**, *76*, 4571–4581.
- [32] J. C. Sciano, *Handbook of Organic Photochemistry*, CRC Press, Boca Raton, FL, **1989**.
- [33] E. M. S. Castanheira, M. S. D. Carvalho, D. J. G. Soares, P. J. G. Coutinho, R. C. Calhelha, M.-J. R. P. Queiroz, *J. Fluoresc.* **2011**, *21*, 911–922.
- [34] C. A. Hunter, K. R. Lawson, J. Perkins, C. J. Urch, *J. Chem. Soc. Perkin Trans. 2* **2001**, 651–669.
- [35] Gaussian 03, Revision C.02, M. J. Frisch, G. W. Trucks, H. B. Schlegel, G. E. Scuseria, M. A. Robb, J. R. Cheeseman, J. A. Montgomery, Jr., T. Vreven, K. N. Kudin, J. C. Burant, J. M. Millam, S. S. Iyengar, J. Tomasi, V. Barone, B. Mennucci, M. Cossi, G. Scalmani, N. Rega, G. A. Petersson, H. Nakatsuji, M. Hada, M. Ehara, K. Toyota, R. Fukuda, J. Hasegawa, M. Ishida, T. Nakajima, Y. Honda, O. Kitao, H. Nakai, M. Klene, X. Li, J. E. Knox, H. P. Hratchian, J. B. Cross, V. Bakken, C. Adamo, J. Jaramillo, R. Gomperts, R. E. Stratmann, O. Yazyev, A. J. Austin, R. Cammi, C. Pomelli, J. W. Ochterski, P. Y. Ayala, K. Morokuma, G. A. Voth, P. Salvador, J. J. Dannenberg, V. G. Zakrzewski, S. Dapprich, A. D. Daniels, M. C. Strain, O. Farkas, D. K. Malick, A. D. Rabuck, K. Raghavachari, J. B. Foresman, J. V. Ortiz, Q. Cui, A. G. Baboul, S. Clifford, J. Cioslowski, B. B. Stefanov, G. Liu, A. Liashenko, P. Piskorz, I. Komaromi, R. L. Martin, D. J. Fox, T. Keith, M. A. Al-Laham, C. Y. Peng, A. Nanayakkara, M. Challacombe, P. M. W. Gill, B. Johnson, W. Chen, M. W. Wong, C. Gonzalez, J. A. Pople, Gaussian, Inc., Wallingford CT, **2004**.
- [36] Y. Miura, E. Yamano, A. Tanaka, J. Yamauchi, *J. Org. Chem.* **1994**, *59*, 3294–3300.
- [37] Programs CrysAlis-CCD and -RED, Oxford Diffraction, Abingdon (UK), **2005**.
- [38] G. M. Sheldrick, SHELX-97, Programs for Crystal Structure Determination (SHELXS) and Refinement (SHELXL), G. M. Sheldrick, *Acta Crystallogr. Sect. A* **2008**, *64*, 112–122.

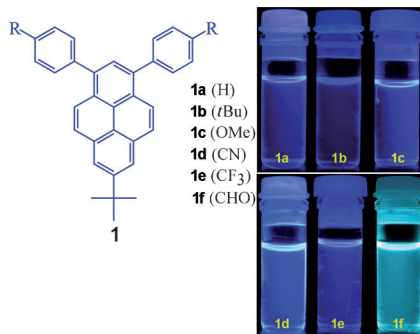
Received: June 13, 2012

Revised: July 25, 2012

Published online: ■■■, 0000

FULL PAPER

Shades of blue: Pyrene-based Y-shaped blue solid-state emitters, 7-*tert*-butyl-1,3-diarylpyrenes **1**, were synthesized by Suzuki cross-coupling reactions in good to excellent yields. Studies on single-crystal X-ray structures and the photophysical properties of these compounds strongly suggest that they are promising blue emitters in organic light-emitting device applications.



Luminescent Compounds

Xing Feng, Jian-Yong Hu,* Liu Yi,
Nobuyuki Seto, Zhu Tao,
Carl Redshaw, Mark R. J. Elsegood,
Takehiko Yamato* ——— ■■■■-■■■■

**Pyrene-Based Y-shaped Solid-State
Blue Emitters: Synthesis, Characteri-
zation, and Photoluminescence**

